



Assimilation of SCIAMACHY total column CO observations: Global and regional analysis of data impact

Andrew Tangborn,^{1,2} Ivanka Stajner,^{1,3} Michael Buchwitz,⁴ Iryna Khlystova,⁴ Steven Pawson,¹ John Burrows,^{4,5} Rynda Hudman,^{6,7} and Philippe Nedelec⁸

Received 15 July 2008; revised 7 January 2009; accepted 28 January 2009; published 10 April 2009.

[1] Carbon monoxide (CO) total column observations from the Scanning Imaging Absorption Spectrometer for Atmospheric Cartography (SCIAMACHY) on board Envisat-1 are assimilated into the Global Modeling and Assimilation Office constituent assimilation system for the period 1 April to 20 December 2004. The impact of the assimilation on CO distribution is evaluated using independent surface flask observations from the National Oceanic and Atmospheric Administration (NOAA)/ESRL global cooperative air sampling network and Measurement of Ozone and Water Vapor by Airbus In-Service Aircraft (MOZAIC) in situ CO profiles. Assimilation of SCIAMACHY data improves agreement of CO assimilation with both of these data sets on both global and regional scales compared to the free-running model. Regional comparisons with MOZAIC profiles made in western Europe, the northeastern United States, and the Arabian Peninsula show improvements at all three locations in the free troposphere and into the boundary layer over Arabia and the northeastern United States. Comparisons with NOAA Earth System Research Laboratory data improve at about two thirds of the surface observation sites. The systematic model errors related to the uncertainty of CO surface sources and the chemistry of CO losses are investigated through experiments with increased surface CO emissions over the Arabian Peninsula and/or globally reduced hydroxyl radical (OH) concentrations. Both model changes decrease mean CO errors at all altitudes in comparison to MOZAIC data over Dubai and Abu Dhabi. In contrast, errors in the assimilated CO are reduced by the increased emissions for pressures ≥ 800 hPa and by the reduced OH for pressures ≤ 600 hPa. Our analysis suggests that CO emissions over Dubai in 2004 are more than double those in the 1998 emissions inventory.

Citation: Tangborn, A., I. Stajner, M. Buchwitz, I. Khlystova, S. Pawson, J. Burrows, R. Hudman, and P. Nedelec (2009), Assimilation of SCIAMACHY total column CO observations: Global and regional analysis of data impact, *J. Geophys. Res.*, *114*, D07307, doi:10.1029/2008JD010781.

1. Introduction

[2] Carbon monoxide (CO) is an important atmospheric trace gas for the global carbon cycle and air quality. The two

largest sources of CO emissions, biomass burning and fossil fuel combustion, are also important sources of carbon dioxide (CO₂) [Pfister *et al.*, 2004]. CO impacts the air quality directly and as a precursor to tropospheric ozone [Berntsen *et al.*, 2005]. CO is primarily lost by reaction with OH and has an atmospheric lifetime of 2 months. Several satellite missions carry instruments that measure radiances at wavelengths sensitive to CO, including the Atmospheric Infrared Sounder (AIRS) [McMillan *et al.*, 2005], Measurements of Pollution in the Troposphere (MOPITT) [Deeter *et al.*, 2003] and the Scanning Imaging Absorption Spectrometer for Atmospheric Cartography (SCIAMACHY) [Buchwitz *et al.*, 2007]. Infrared AIRS and MOPITT radiances are most sensitive to CO between pressures of 400 and 700 hPa. SCIAMACHY CO is retrieved from reflected solar radiation in the near infrared band 2324–2335 nm, which is sensitive to variations within the boundary layer. This sensitivity can potentially play an important role in forecasting ground level air quality and inverting for emissions sources.

¹Global Modeling and Assimilation Office, Goddard Space Flight Center, Greenbelt, Maryland, USA.

²Also at Joint Center for Earth Systems Technology, University of Maryland, Baltimore County, Baltimore, Maryland, USA.

³Now at Noblis, Inc., Falls Church, Virginia, USA.

⁴Institute of Environmental Physics, University of Bremen, Bremen, Germany.

⁵Also at Centre for Ecology and Hydrology, Wallingford, Oxfordshire, UK.

⁶Atmospheric Chemistry Modeling Group, Harvard University, Cambridge, Massachusetts, USA.

⁷Now at College of Chemistry, University of California, Berkeley, California, USA.

⁸Laboratoire d'Aérodynamique, Université de Toulouse, CNRS, Toulouse, France.

[3] Chemical constituent data assimilation involves combining observations with model forecasts in order to improve estimation of the constituent distribution or sources (in the case of chemical inversion). Assimilation provides a useful tool to evaluate the accuracy of retrieved satellite data relative to models or other measurements. Total column measurements cannot be directly compared with in situ point observations without knowledge of the complete atmospheric profile. Three-dimensional analyzed constituent fields can provide a transfer standard [e.g., *Lahoz et al.*, 2007] for indirect comparisons since they can be judged against both the total column and in situ observations. If the analysis fields are drawn closer to highly accurate independent data as a result of assimilating satellite observations, this gives a strong indication that the latter provide useful information. When direct measurements of CO profiles are available, the correction made through assimilating total column observations from a satellite can be evaluated in terms of whether CO is added (or removed) in the appropriate model level.

[4] Assimilation of CO observations has been undertaken by a number of researchers using measurements from several different infrared sounders. These include the Measurement of Air Pollution from Space (MAPS) [*Lamarque et al.*, 1999]; Interferometric Monitor for Greenhouse Gases (IMG) [*Clerbaux et al.*, 2001] and MOPITT [*Lamarque et al.*, 2004; *Yudin et al.*, 2004]. The assimilated CO fields were compared to independent observations in only some of these systems, the biggest improvements are generally near the midtroposphere where the averaging kernels peak. In contrast, *Zubrow et al.* [2008] assimilated surface observations from the Environmental Protection Agency (EPA) into a regional model, and consistently found a large reduction in errors relative to independent surface data. However, no comparisons were made with CO measurements aloft so the impact of the assimilation to free tropospheric CO is unknown. SCIAMACHY sensitivity to CO in the boundary layer and free atmosphere offers potential for improvements in estimating CO throughout the troposphere.

[5] In this paper we assess the impact of SCIAMACHY total column CO observations on the CO assimilation system developed at the Global Modeling and Assimilation Office (GMAO). This system uses meteorological analyses from the Goddard Earth Observing System (GEOS), Version 4 [*Bloom et al.*, 2005; *Stajner et al.*, 2008] to transport CO. The assimilation is evaluated using the National Oceanic and Atmospheric Administration (NOAA)/ESRL global cooperative air sampling network [*Novelli et al.*, 2003] and in situ observations from the Measurement of Ozone, Water Vapor, Carbon Monoxide, and Nitrogen Oxides by Airbus In-Service Aircraft (MOZAIC) observing system [*Nedelec et al.*, 2003]. We investigate where assimilation of SCIAMACHY observations leads to the greatest improvements to CO estimation, and what information the assimilation and comparisons with in situ data can provide about the source of errors in the model. The assimilation system is run for the period 1 April to 20 December 2004. The comparisons with NOAA/ESRL and MOZAIC data is done from May through December.

2. SCIAMACHY Observations

[6] The SCIAMACHY instrument has been operating on board the environmental satellite, Envisat-1, of the European

Space Agency (ESA) since March 2002. The SCIAMACHY observations are retrieved from nadir measurements in the 2265–2380 nm spectral range, and have a typical horizontal resolution of 120 km across track and 30 km along track. The measurements exhibit seasonal variability expected in global CO fields [*Buchwitz et al.*, 2007]. Comparisons were made with MOPITT, which showed an agreement within roughly 20% without taking into account the differences in sensitivity with altitude. Figure 1 shows a set of 3-month averaged total column CO from SCIAMACHY for the year 2004. These indicate hemispheric differences and large-scale seasonal patterns, such as biomass burning over South America and Africa, which are qualitatively consistent with MOPITT observations [*Bremer et al.*, 2004].

[7] Retrievals of total column CO (denoted c_{tc}°) use the Weighting Function Modified–Differential Optical Absorption Spectroscopy (WFM-DOAS) algorithm. WFM-DOAS is a least squares technique that uses the scaling and shifting of preselected vertical profiles to fit the ratio of the measured nadir radiance to the solar irradiance spectrum [*Buchwitz et al.*, 2007]. This approach is valid only for cloud-free pixels, and a cloud detection algorithm using subpixel information generates a cloud mask. The SCIAMACHY c_{tc}° observations are supplied with a cloud contamination flag, as well as a quality flag, which depends on the magnitude of the residual of the least squares fit for each retrieval. The estimated observation error for each total column measurement, σ_{scia}° , is calculated from the RMS of the residual and contains contributions from both random and (unknown) systematic components. These total error values generally range from 20% to 100% for the observations tagged as “good.” These error estimates can be verified through data assimilation, and this is one of the goals of this work. Only the cloud-free, “good” quality data are used in the assimilation.

[8] The sensitivity of measured radiation to variations in CO at different levels in the atmosphere is characterized by the vertical column averaging kernels (Figure 2a) [*Buchwitz et al.*, 2004]. The averaging kernels depend significantly on the SZA if it is larger than 75° . This is due to the enhanced atmospheric scattering at larger path length. For SZA below 75° , the averaging kernels are essentially constant and very close to unity. This indicates that SCIAMACHY can observe enhancements of CO molecules independent of the altitude where the enhancement occurs.

[9] Only data for SZA $< 75^{\circ}$, whose averaging kernels very close to unity, are assimilated. Note that there is slightly more sensitivity to concentrations near 300 hPa than in the lower Troposphere and that the near-surface sensitivity decreases as solar zenith angle increases. There is also some dependence of the averaging kernel on surface reflectivity.

3. Assimilation System

[10] The CO assimilation system used here is based on the ozone assimilation system developed by *Stajner et al.* [2001, 2008] and employs the sequential Physical-space Statistical Analysis System (PSAS) [*Cohn et al.*, 1998], which is an alternative formulation of 3DVAR. The CO data assimilation system has the capability to include the effect of the averaging kernel, which takes into account vertical variations of the sensitivity of the retrieved to actual CO mixing ratios. Because we limit the observations to those with the

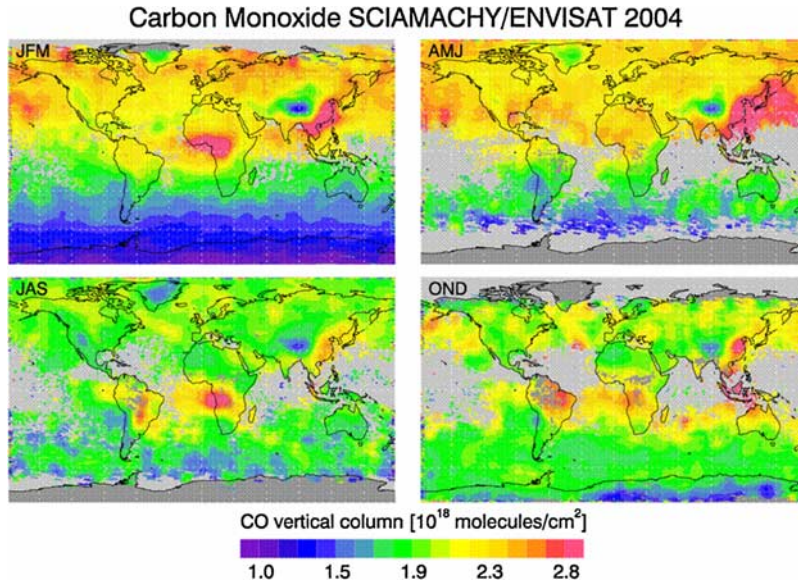


Figure 1. Total column CO from Scanning Imaging Absorption Spectrometer for Atmospheric Cartography (SCIAMACHY) averaged over 3-month periods during 2004, plotted on a $0.5^\circ \times 0.5^\circ$ grid. Typical data density is about 24 observations per box over each 3-month period, though we only plot the observations flagged as “good.” Plots are for (top left) January–February–March, (top right) April–May–June, (bottom left) July–August–September, and (bottom right) October–November–December.

averaging kernels near unity, the forward (or observation) operator from model space to total column observation space is simply a weighted vertical integration. The a priori profile that was used in SCIAMACHY retrievals is subtracted out within each layer, and the total column a priori is added to the final result. For a profile \mathbf{x} given on $N = 55$ model levels by volumetric mixing ratios x_k , $k = 1, \dots, N$ in mol/mol, we introduce the linear operator $H(\mathbf{x})$:

$$H(\mathbf{x}) = 2.12 \times 10^{22} \sum_{k=1}^N a_k (\Delta P_k) x_k, \quad (1)$$

where a_k is the SCIAMACHY averaging kernel, ΔP_k is the k^{th} layer pressure thickness (hPa). The constant (2.12×10^{22}) converts the total column value to molecules/ cm^2 . In our application $a_k = 1$ (see Figure 2a). The total column operator that computes the total column CO in molecules/ cm^2 is

$$\mathcal{H}(\mathbf{x}) = H(\mathbf{x} - \mathbf{x}^{ap}) + c_{tc}^{ap}, \quad (2)$$

where \mathbf{x}^{ap} is the a priori CO mixing ratio on model levels and c_{tc}^{ap} is the total column a priori.

[11] Equation (2) defines the observation operator that allows for the calculation of the observed minus forecast (O – F), or innovation, values in observation space needed for the assimilation system. These represent the difference between the observation and forecast, and their magnitude and sign play an important role in how the assimilation changes the constituent field. The PSAS algorithm solves the innovation equation

$$(\mathbf{H}^f \mathbf{H}^T + \mathbf{R})\mathbf{y} = (\mathbf{c}_{tc}^o - \mathcal{H}(\mathbf{x}^f)) \quad (3)$$

for the vector \mathbf{y} , in observation space. The observation operator, \mathbf{H} , is the matrix of the linear operator in equation (1) and error statistics are represented by the forecast error covariance, \mathbf{P}^f . The observation error covariance, \mathbf{R} is a diagonal matrix made up of observation error variances, implying that the observation errors are modeled as uncorrelated.

[12] The solution is then transformed to model space via

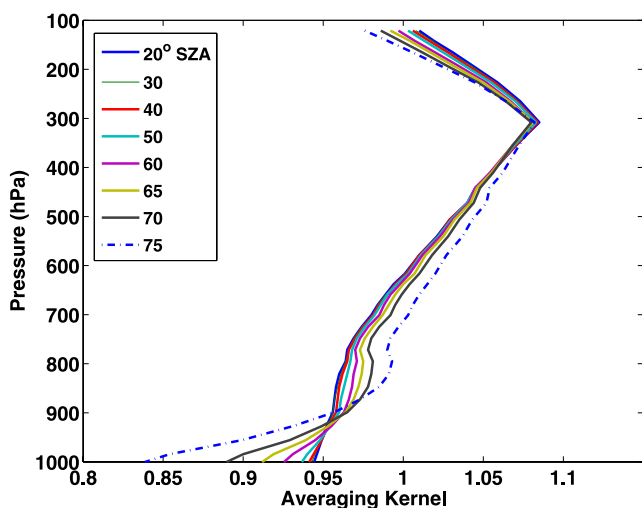
$$\mathbf{x}^a - \mathbf{x}^f = \mathbf{P}^f \mathbf{H}^T \mathbf{y} \quad (4)$$

to obtain the analysis increment $\mathbf{x}^a - \mathbf{x}^f$, where \mathbf{x}^a is the CO analysis and \mathbf{x}^f is the CO forecast.

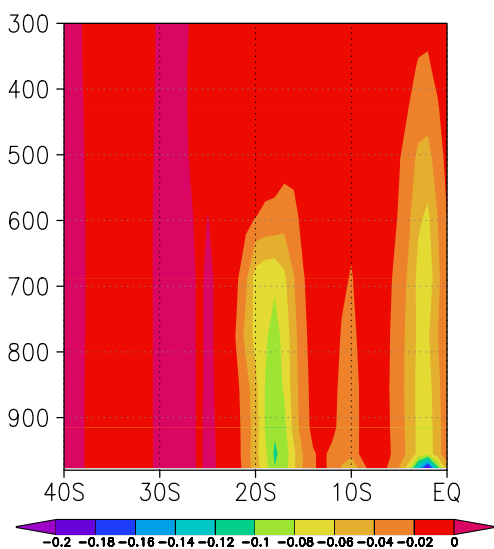
[13] The forecast error covariance is specified using a separable covariance model [Stajner *et al.*, 2001]:

$$\{P_{ij}\} = \sigma_i \sigma_j \rho_{ij} \mu_{ij}, \quad (5)$$

where $\{P_{ij}\}$ is the covariance between locations i and j , σ_i and σ_j are the forecast error standard deviations, ρ_{ij} is a nonisotropic horizontal error correlation and μ_{ij} is the vertical error correlation. Three tunable parameters are used in the error covariance models: α specifies the forecast error standard deviation as a fraction of the local CO mixing ratio, $\sigma^f = \alpha \mathbf{x}^f$, L is the background error correlation length scale, and β is used to specify observation error standard deviation $\sigma^o = \beta \sigma^{\text{scia}}$. Tuning runs were used to determine optimal values (by minimizing the RMS difference with MOZAIC observations): $\alpha = 0.2$ and $\beta = 0.5$. The optimal horizontal correlation length scale was found to be 100 km in the meridional direction, and varies from 200 km in the Tropics to 100 km in high latitudes for the zonal direction. A χ^2 estimate [see Stajner *et al.*, 2001], normalized with respect to the number of SCIAMACHY observations at



(a)



(b)

Figure 2. (a) The SCIAMACHY CO averaging kernel (dimensionless) at various solar zenith angles and (b) analysis increment at 25E over southern Africa on 30 September 2004. Units are ppmv.

each analysis time was also made for each tuning run. This normalized mean is closest to unity (0.99) for the same choice of parameters that provide the best agreement with MOZAIC data.

[14] These parameter values are used in all the assimilation experiments presented in the next section. The value of β implies that the observation errors provided with the CO retrievals are too large (relative to the MOZAIC observations), possibly due to an overestimation of the systematic component of the error.

[15] The CO forecasts are produced online in the GEOS-4 GCM, with parameterized chemistry and imposed sources. The GCM uses the semi-Lagrangian transport finite volume scheme [Lin, 2004] with 55 levels between the surface and 0.1 hPa. The meteorological analyses are generated using the GEOS-4 assimilation system [Bloom et al., 2005], and

are then utilized for 6-h GCM runs which drive the constituent transport. Meteorological and constituent fields are computed on a 1° latitude by 1.25° longitude grid. The model is employed in two ways. First, it is used to produce a CO model run, in which CO transport is constrained by the GEOS-4 meteorological analyses. This run is called the “CO simulation,” and it provides a benchmark to compare with the assimilation results. Second, the model is used to forecast CO (provide the background fields) for the “CO assimilation,” in which the SCIAMACHY observations are inserted every 6 h to provide new initial conditions (analyses). Transport fields (winds and cloud convection) are identical in the two runs.

[16] The CO production rate (P) and loss frequencies (L) are taken from the GEOS-CHEM model global 3-D model of tropospheric chemistry. Monthly mean climatological hydroxyl radical (OH) concentration is used to specify CO destruction. The treatment of OH fields as independent of reaction with CO is justified by the abundant sources of OH in the atmosphere [Duncan et al., 2000]. The net rate of change in CO mixing ratio on the model grid is then

$$\frac{\partial[\text{CO}]}{\partial t} = P - L[\text{CO}]. \quad (6)$$

A general description of GEOS-Chem is given by *Bey et al.* [2001] and a specific description of emissions as used here is given by *Park et al.* [2004], with modifications described here. Anthropogenic emissions over the United States are from the 1999 National Emission Inventory (NEI) with modifications described by *Hudman et al.* [2007], including a generalized 50% decrease in NO_x emissions from power plants and industry reflecting documented changes between 1999–2004, and a 30% decrease in CO emissions to account for overestimate in the transport sector [Parrish, 2006]. Biomass burning emissions are climatological means as described by *Duncan et al.* [2003], with the addition of fire emissions over North America following *Turquetty et al.* [2007], which provided them an unbiased comparison with MOPITT CO observations over summer 2004. Boreal fire emissions are assigned to both the boundary layer and free troposphere so as to account for the convection generated by the fires.

4. Assimilation Results

[17] The impact of SCIAMACHY data for a single analysis time can be seen in Figure 2b in a vertical slice of the analysis increment (analysis minus forecast) at 25° E and 1800 UT on 30 September 2004. This increment includes a number of observations, and the most substantial corrections correspond to three observations in or near the plane of this plot at 18°S , 10°S , and 2°S . The corrections extend through a deep layer and maximize at the surface. This vertical structure is due to the assumption that the forecast error standard deviation is proportional to the local CO mixing ratio, which is typically highest in the boundary layer. The shape of the SCIAMACHY analysis increments contrasts with the shape of MOPITT increments, which tend to peak around 500 hPa, and then decay toward the surface [Lamarque et al., 2004], echoing the different shapes of the averaging kernels.

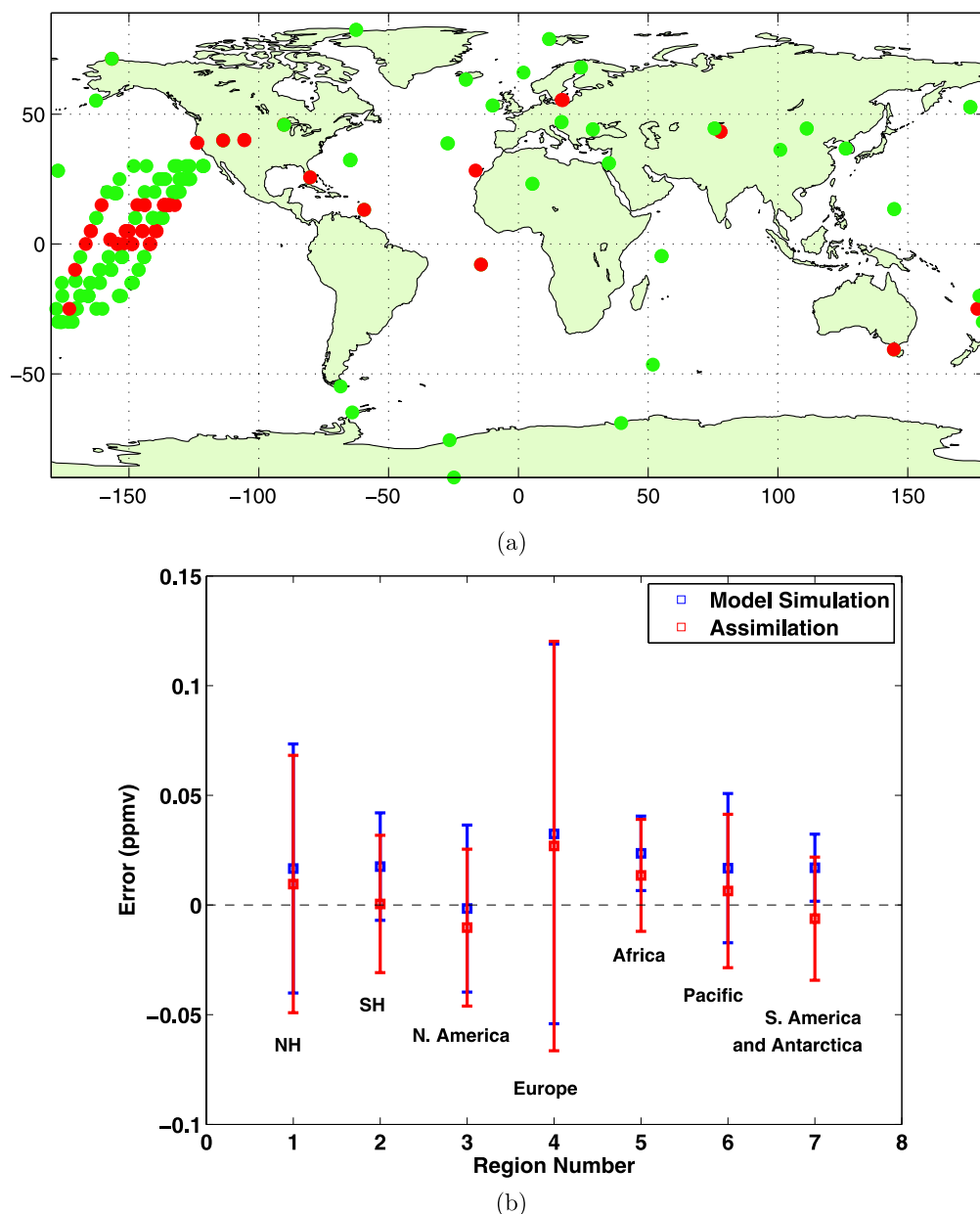
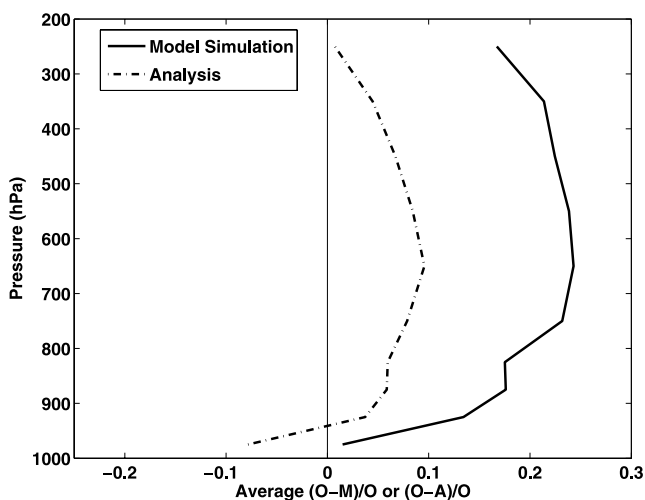


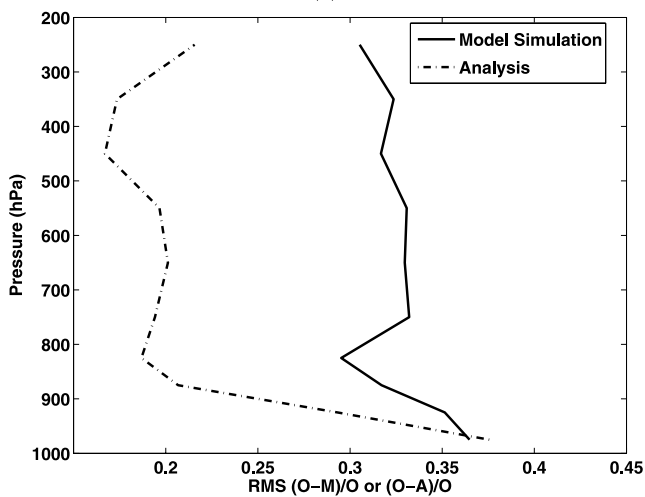
Figure 3. Comparison of model simulation and assimilation with National Oceanic and Atmospheric Administration/ESRL surface flask data during the period May–December 2004. (a) A map of the measurement locations with the change in mean error relative to the in situ data given by a green dot when the assimilation errors are lower and a red dot when the CO simulation errors are lower. (b) The magnitude of these changes which gives the mean and standard deviation errors relative to the in situ measurements. The CO simulation errors are indicated by the blue lines, and the assimilation errors are indicated by the red lines.

[18] Global and regional comparisons with NOAA/ESRL flask data and MOZAIC observations are used to evaluate model performance and impact of SCIAMACHY data during the period 1 May to 20 December 2004. The locations of the 276 NOAA/ESRL measurements and the impact of SCIAMACHY assimilation on the mean analysis error are shown in Figure 3a. The green dots represent locations where the mean analysis error has been reduced by assimilation of SCIAMACHY, and the red dots indicate where it has increased. Most regions show decreases in error, with

the notable exceptions of the western United States, and parts of the equatorial Pacific. These changes can be seen quantitatively in Figure 3b, in which the locations are divided into Northern Hemisphere (NH), Southern Hemisphere (SH), and also into five subregions. For each region, the plot shows the mean error for the CO simulation (blue square) and the Assimilation (red square). The error standard deviation is also shown for each region using error bars. The mean differences were reduced in both the NH and SH, and all of the subregions except North America. In



(a)



(b)

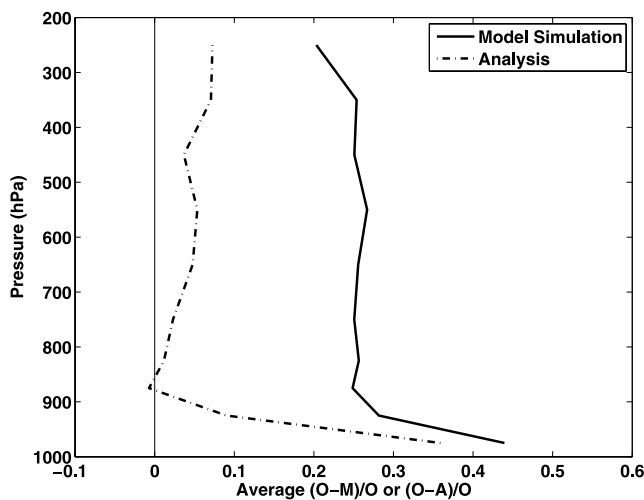
Figure 4. Relative (a) mean and (b) RMS $O - A$ in the box containing Measurement of Ozone and Water Vapor by Airbus In-Service Aircraft (MOZAIC) observations within 5° longitude or latitude of Frankfurt, where “O” refers to the MOZAIC observations, “A” to the analysis field, and “M” to the CO simulations interpolated to MOZAIC locations. Solid lines refer to the CO simulation ($(O - M)/O$ average; RMS $((O - M)/O)$) and dash-dotted lines refer to the CO assimilation ($(O - A)/O$ average; RMS $((O - A)/O)$).

North America, the mean model error was essentially zero making any improvement difficult. In contrast, the standard deviation of the differences from flask data are generally larger when SCIAMACHY observations are assimilated. This is because the variability of the surface layer CO fields has been increased, since the assimilation creates a sudden change to the field which gradually returns toward the CO simulation state due to model biases.

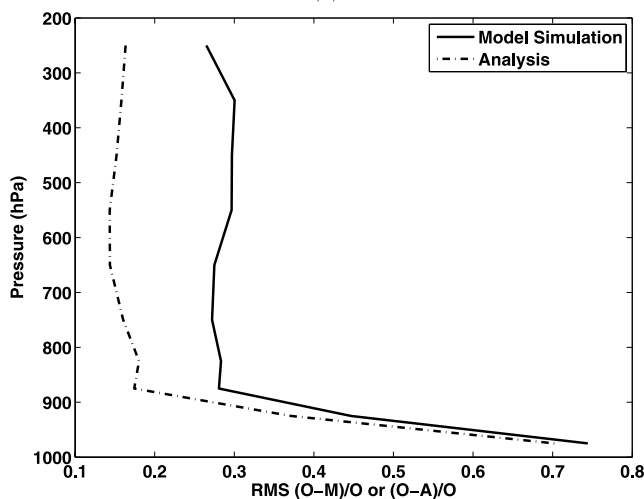
[19] Regional comparisons with MOZAIC data focus on three 10° latitude \times 10° longitude boxes centered near Frankfurt, Germany; New York, USA; and Dubai, UAE. Separating the comparisons with independent data in this manner allows us to consider the impact of the geographic variability of the accuracy of the source estimates on the

assimilation. Jet takeoffs and landings in each region provide CO profiles numbering from around 35 (Dubai and Abu Dhabi) to about 500 (Frankfurt) from near sea level to about 200 hPa for the period from 1 May to 20 December 2004. Note that the nature of MOZAIC observations means that spatial coverage and temporal sampling have large geographical differences [Nedelec et al., 1998].

[20] Comparisons of the mean and root-mean-square (RMS) differences between MOZAIC observations and the CO simulation reveal that CO values in the model are generally too low at pressures lower than 700 hPa. At higher pressures the model errors depend more strongly on geographical location, and for this reason we focus on regional comparisons. Figures 4–6 show the relative mean and RMS of the difference between the MOZAIC observations and the CO simulation (solid line) or CO assimilation (dash-dotted line) interpolated to the MOZAIC observation locations within the boxes centered on Frankfurt (Germany), Dubai (United Arab Emirates) and New York City (United States), respectively. Profiles over Dubai show larger errors than over New York or Frankfurt. The improvement is particularly large near Dubai, where larger analysis increments counteract



(a)



(b)

Figure 5. Same as Figure 4, but for Dubai.

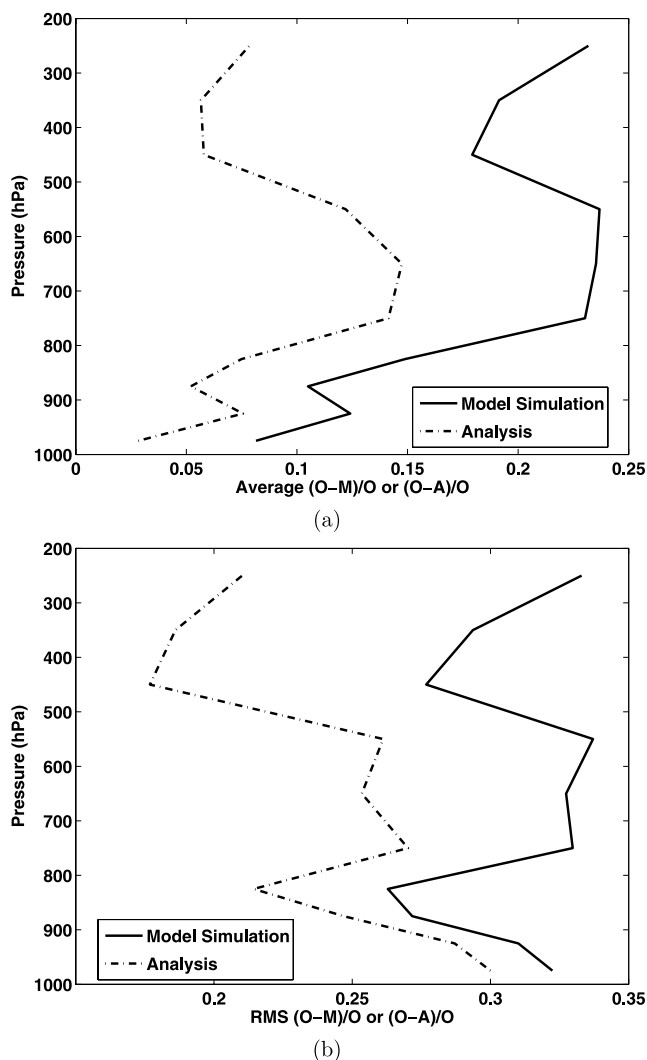


Figure 6. Same as Figure 4, but for New York City.

large model errors. For example, the mean error reduction above Dubai varies from 40% at the surface to 100% just above the boundary layer. Over New York, the reduction is around 50% at all levels. In contrast, the mean errors near Frankfurt are essentially unchanged by the assimilation in the surface layer. The mean error in the upper troposphere is substantially reduced by the assimilation over all three cities. Assimilation of SCIAMACHY data provides closer agreement with MOZAIC CO globally (not shown).

[21] Similarly, the RMS errors show a reduction at all levels only over Dubai, where the decrease varies from 10% at the surface to about 50% in the upper troposphere. RMS reduction over New York varies from 10% (surface) to 30% (upper troposphere). Above Frankfurt, reduction occurs only at pressures below 900 hPa, with a maximum reduction of about 30%. In all three locations, and for pressures lower than 900 hPa, the analysis RMS errors vary from 15% to 30%. The forecast RMS errors (not shown) are very similar in magnitude to the analysis RMS errors, indicating that the estimated forecast error of 20% of the CO mixing ratio is reasonable outside the boundary layer. Over Dubai, assimilation of SCIAMACHY data decreases mean and RMS

differences with MOZAIC data in the boundary layer. Over the Arabian Peninsula, favorable conditions for the assimilation include the frequent availability of cloud-free SCIAMACHY data and the fact that the model consistently underestimates CO in the boundary layer and in the total columns. The former allows frequent corrections due to the assimilation and the latter ensures that the distribution of analysis increments in the vertical helps improve the representation of CO in the boundary layer. Assimilation of SCIAMACHY data leads to a consistent large decrease in the RMS differences with MOZAIC data globally and in all three regions between about 200 and 700 hPa. At these levels, which are away from the immediate impact of errors in CO sources (see Figure 2b), the impact of the analysis increments can accumulate to produce these substantial corrections.

[22] The height-dependent impact of assimilating SCIAMACHY can be seen in Figure 7, which shows the difference between the CO assimilation and CO simulation (A–M) averaged over September and October 2004 for the three regions studied. Each plot is for a vertical slice from the surface to 200 hPa at a latitude that runs through Frankfurt

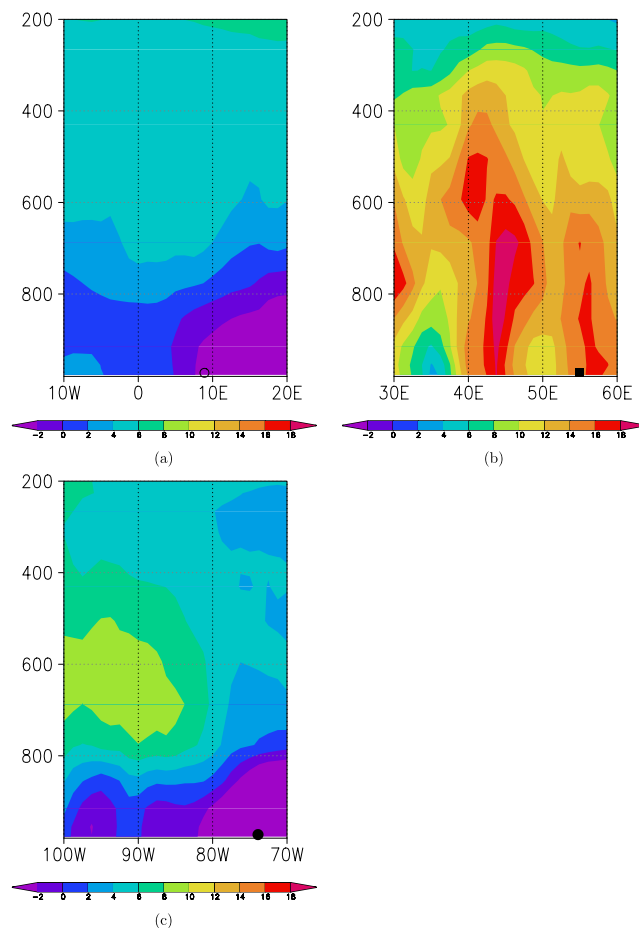


Figure 7. Difference between CO assimilation and CO simulation in parts per billion by volume, averaged over the period 1 September to 31 October 2004 for vertical slices at (a) 51°N, spanning Frankfurt, denoted by an open circle; (b) 25°N, spanning Dubai, denoted by a square; and (c) 41°N, spanning New York, denoted by a solid circle.

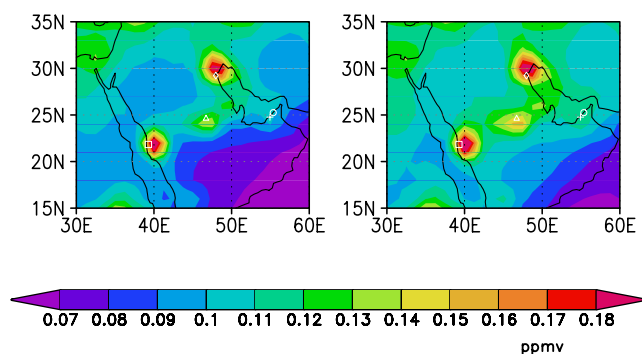


Figure 8. CO field in parts per million by volume for the lowest model layer averaged over the period 1 September to 31 October 2004 for the (left) CO simulation and (right) CO assimilation using cloud-free observations in the Middle East. The cities marked are Kuwait City (diamond), Jeddah (square), Riyadh (triangle), Abu Dhabi (cross), and Dubai (circle).

(a), Dubai (b) or New York (c). In the Frankfurt and New York regions, the corrections are positive at pressures lower than 800 hPa, and negative near the surface. Analysis increments from the assimilated SCIAMACHY observations will generally be of the same sign at all levels (Figure 2b). Over Frankfurt and New York, this means that the changes made in the upper troposphere CO cannot be the result of the same observations as the changes seen at the surface. This indicates that the upper tropospheric changes result from corrections made elsewhere and transported to these regions. An example of this is the upper level increase in CO over New York. The small changes nearer the surface can be attributed to some combination of a more accurate emissions model, and a relatively small number of cloud-free observations. The negative surface correction is also consistent comparisons with ICARTT made by *Hudman et al.* [2008] that indicated that CO emissions over the U.S. should be reduced in the model. Above the Arabian Peninsula the assimilation changes the CO field in a much different way; the corrections are positive right down to the surface, and have the appearance of “plumes” above Riyadh and Dubai. These are really corrections to the CO field over the two cities, and they suggest that the specified CO sources are too low in this region. The corrections to CO over Dubai might then be interpreted as the response of the assimilation to locally underestimated sources.

[23] Because assimilation of SCIAMACHY CO results in correction to the CO field throughout the troposphere, it is interesting to plot the surface layer CO fields in the Arabian Peninsula. Figure 8 shows the average fields for September–October 2004 in this region. The assimilation increases surface layer CO throughout the peninsula. This indicates a substantial underestimation of CO surface layer concentration in the model. In particular, the concentrations around the two largest sources, Kuwait city and Jeddah, increase substantially. The only two cities with MOZAIC data in the Arabian Peninsula region during this time period are Dubai and Abu Dhabi, and there the increase in CO due to the assimilation improves the agreement with MOZAIC data (Figure 5). Two possible causes for low bias in the model are considered: underestimated CO surface sources and

overestimated CO loss due to its reaction with OH aloft. The former would tend to create errors nearer the surface, while the latter should result in larger errors outside the boundary layer. Chemical loss of CO from oxidation by OH is slow relative to boundary layer ventilation and is therefore of little consequence.

[24] Additional experiments provide insight on how the model and assimilation respond to changes in emissions and/or OH concentrations. Doubling the CO emissions in the Arabian Peninsula increased CO (and reduced errors) at all levels in the free running model, but only for pressures above 800 hPa in the assimilation. Similarly, a global 10% reduction in OH reduced errors at all levels in the CO simulation, but only upper tropospheric errors ($p < 600$ hPa) were reduced in the assimilation. We show the mean errors with and without these changes to emission and global OH in Figure 9. Combining increased Arabian emission with a global 10% decrease in OH provides the best agreement with MOZAIC data for the CO simulation at all levels and the assimilation at pressures below 600 hPa and above 900 hPa. At the surface in Dubai, doubled regional emissions and globally 10% reduced OH decrease the mean error in the CO simulation relative to MOZAIC by about 30% (from 0.39 to 0.27 ppmv). Note that the assimilation of SCIAMACHY data into this model further reduces the error by about 50% (from 0.27 to 0.13 ppmv), as can be seen from the change in the red line from Figures 9a and 9b. This relative error reduction is very similar to the improvement from assimilation of SCIAMACHY into the original model (Figure 5).

[25] The spatial impact of these changes to the chemistry model can be seen in Figure 10, which shows the total column differences between SCIAMACHY observations and CO simulations averaged over the month of October 2004, using standard chemistry (Figure 10a) and chemistry with doubled Middle East emissions and OH reduced globally by 10% (Figure 10b). These plots indicate that the higher levels of CO that result from this modified chemistry draw the total column CO closer to SCIAMACHY observations. For example in the region near Dubai and Abu Dhabi (where the MOZAIC profile measurements are made), the total column differences are reduced from about 1.0×10^{18} molecules/cm² to about 0.6×10^{18} molecules/cm². Total column O – F values for the assimilation run using both the original and enhanced chemistry (not shown) are smaller than those in Figure 10 and show little dependence on the chemistry model used. This is due to the fact that the assimilation draws the CO total columns strongly toward the observed values.

5. Concluding Remarks

[26] The assimilation of SCIAMACHY total column CO observations is found to draw the CO assimilation closer to an independent data set both globally and in the localized regions of the northeastern United States, the Arabian Peninsula and western Europe. The mean errors of surface CO were reduced at about two-thirds of the NOAA/ESRL flask data sites, and were improved overall in all of the regions except North America, where the mean error in the model is the smallest of all regions. The mean CO mixing ratio is drawn toward MOZAIC profiles from 200 hPa down

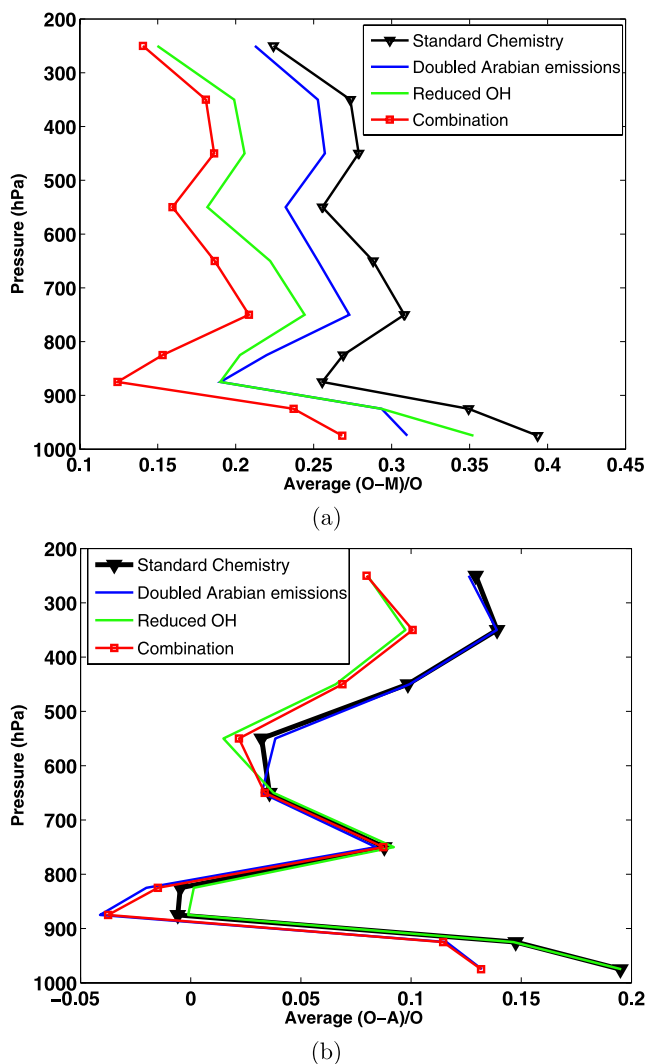


Figure 9. Relative mean (a) $O - M$ and (b) $O - A$ in the box containing MOZAIC observations within 5° longitude or latitude of Dubai, where “O” refers to the MOZAIC observations, “M” refers to the free model run, and “A” is the analysis field interpolated to MOZAIC locations. The black lines (with triangles) use the standard (GEOS-CHEM) anthropogenic emissions, the blue lines use a chemistry model with doubled CO emission in the Arabian Peninsula, the green lines contain a 10% global reduction in OH, and the red lines (with squares) use both model adjustments.

to the surface at both Dubai and NYC. RMS differences with MOZAIC are also substantially reduced by the assimilation, with only the lowest layer over Frankfurt showing no improvement. Reasons for the lack of improvement in the surface layer over Frankfurt are the very low systematic error in the model over Europe and the relatively smaller number of cloud-free observations there (only half that for a similar sized region in the Middle East). We conclude that SCIAMACHY observations are most useful in regions with frequent cloud-free days, and particularly when the CO production in the model is less accurate. For example, mean surface errors over Dubai (which had roughly twice as many

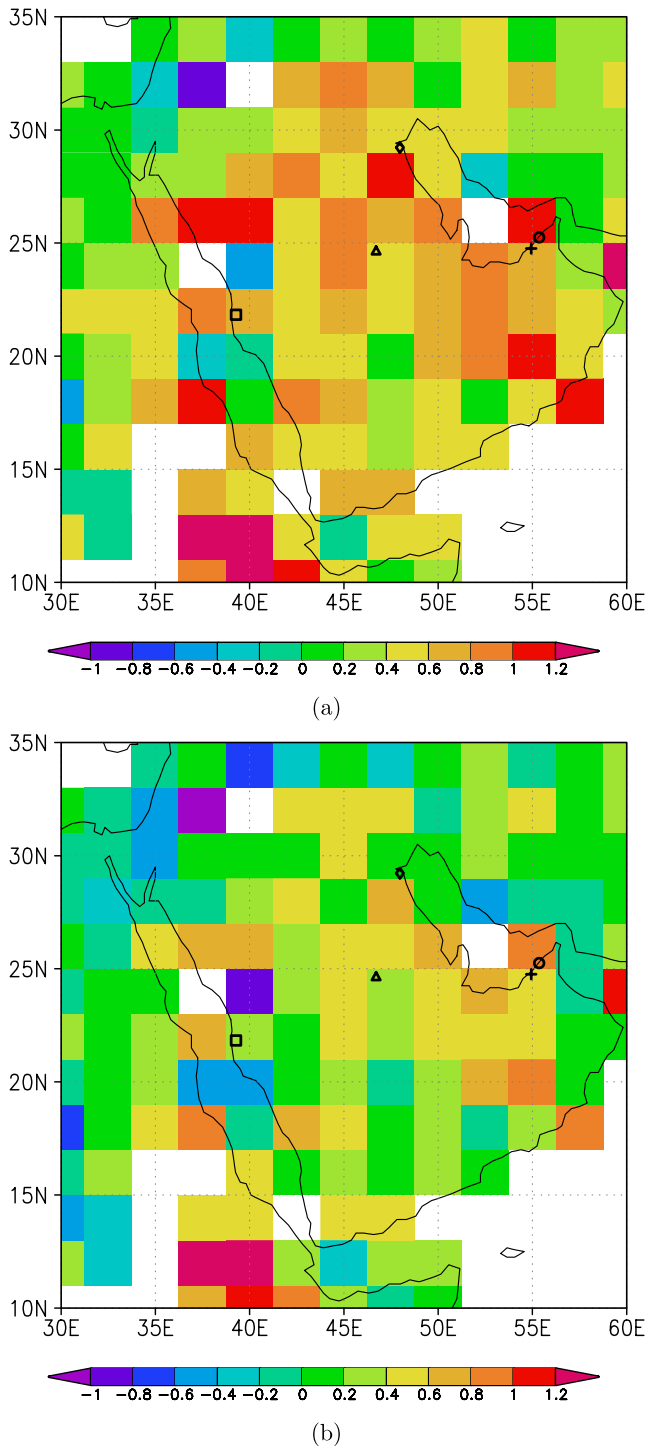


Figure 10. Total column differences between observed and simulated values ($\text{molecules}/\text{cm}^2/1.0 \times 10^{18}$) averaged over the month of October 2004 for the Arabian Peninsula using (a) standard chemistry and (b) doubled Middle East emissions and a global 10% reduction in OH. Symbols for cities are the same as in Figure 8. Red squares indicate positive differences, green indicates differences close to zero, and blue indicates negative differences.

cloud-free observations than the region near Frankfurt) were reduced by about 30%. The observations have less impact in regions with more accurate CO sources or with fewer cloud-free SCIAMACHY observations. The RMS errors in the assimilation show that the assumption of a forecast error standard deviation of about 20% is justifiable in the free troposphere. Nearer the surface, it is more reasonable to consider the mean $O - A$ values (because of subgrid variability in the MOZAIC data), and these indicate that the surface layer forecast errors have substantial spatial variability, and that future improvements to any CO assimilation system would need to take this into account.

[27] Assimilation experiments reveal that SCIAMACHY total column observation error standard deviations may be 50% smaller than the values obtained from the retrieval error estimates. The observation error can be decomposed into random and systematic components. The former represents measurement accuracy and cannot be reduced, while the latter represents the systematic component, and is more likely to be overestimated.

[28] The basic driving force behind data assimilation is the observation minus forecast, or ($O - F$), which represents the difference between the total columns of CO as seen by the satellite and predicted by the model. These ($O - F$) values represent the sum of forecast and observation errors, without explicit information on which error source predominates, or what level in the atmosphere should be corrected the most. This partition is specified through the error covariance estimates and the averaging kernel. For SCIAMACHY, it results in corrections to the CO field that occur at all levels in the troposphere.

[29] Over the Arabian Peninsula, assimilation of SCIAMACHY data has a large impact on the CO field, which improves comparisons with MOZAIC data (Figure 5). Apparently large model errors in this region motivated sensitivity experiments to investigate their origin. The errors in the CO field relative to MOZAIC data decrease substantially in CO simulation experiments with enhanced CO emissions over the Arabian Peninsula and/or global reduction of OH, indicating that both are important components of the model errors in this region. Even after these changes in the model, the assimilation of SCIAMACHY data further reduces CO errors near the surface by about 50% over Dubai. This indicates the robustness of the beneficial impact of SCIAMACHY data. Other components of the model error that could be investigated in the future include errors in the boundary layer height (which impact mixing of CO into the free Troposphere), parametrization of the convective transport [e.g., Ott et al., 2009] and underestimation of distant or unspecified CO surface emissions [e.g., Kar et al., 2006].

[30] **Acknowledgments.** This project was funded in the GMAO under NASA NRA-03-OES-02 (carbon cycle research) and a NASA Modeling Analysis and Prediction (MAP) grant. Computing resources were provided by NASA's High-End Computing Program at GSFC. Funding for the University of Bremen came from DLR-Bonn (grant 50EE0727), ESA (PROMOTE), and the EU (AMFIC). The authors acknowledge the strong support of the European Communities, Airbus, and the airlines Lufthansa, Austrian, and Air France, who carry the MOZAIC equipment free of charge and have performed maintenance since 1994. We also gratefully acknowledge the contribution of Paul Novelli, who made available the CO flask data from the NOAA/ESRL global cooperative air sampling network. The comments from the three anonymous reviewers greatly helped to improve the quality of the manuscript.

References

- Berntsen, T. K., J. S. Fuglestedt, M. M. Joshi, K. P. Shine, N. Stuber, M. Ponater, R. Sausen, D. A. Hauglustaine, and L. Li (2005), Response of climate to regional emissions of ozone precursors: Sensitivities and warming potentials, *Tellus, Ser. B*, *57*, 283–304.
- Bey, I., D. J. Jacob, R. M. Yantosca, J. A. Logan, B. D. Field, A. M. Fiore, Q. Li, H. Y. Liu, L. J. Mickley, and M. G. Schultz (2001), Global modeling of tropospheric chemistry with assimilated meteorology: Model description and evaluation, *J. Geophys. Res.*, *106*, 23,073–23,095.
- Bloom, S. C., A. M. da Silva, D. P. Dee, M. Bosilovich, J.-D. Chern, S. Pawson, S. Schubert, M. Sienkiewicz, W.-W. Tan, and M.-L. Wu (2005), Documentation and validation of the Goddard Earth Observing System (GEOS) Data Assimilation System (DAS)—Version 4, *NASA Tech. Rep.*, 104606, 26 pp.
- Bremer, H., et al. (2004), The spatial and temporal variation of MOPITT CO in Africa and South America: A comparison with SHADOZ ozone and MOIDS aerosol, *J. Geophys. Res.*, *109*, D12304, doi:10.1029/2003JD004234.
- Buchwitz, M., R. de Beek, K. Bramstedt, S. Noël, H. Bovensmann, and J. P. Burrows (2004), Global carbon monoxide as retrieved from SCIAMACHY by WFM-DOAS, *Atmos. Chem. Phys.*, *4*, 1954–1960.
- Buchwitz, M., I. Khlystova, H. Bovensmann, and J. P. Burrows (2007), Three years of global carbon monoxide from SCIAMACHY: Comparison with MOPITT and first results related to the detection of enhanced CO over cities, *Atmos. Chem. Phys.*, *7*, 2399–2411.
- Clerbaux, C., J. Hadji-Lazaro, D. Hauglustaine, and G. Mégie (2001), Assimilation of carbon monoxide measured from satellite in a three-dimensional chemistry-transport model, *J. Geophys. Res.*, *106*, 15,385–15,394.
- Cohn, S. E., A. da Silva, J. Guo, M. Sienkiewicz, and D. Lamich (1998), Assessing the effects of data selection with the DAO physical-space statistical analysis system, *Mon. Weather Rev.*, *126*, 2913–2926.
- Deeter, M. N., et al. (2003), Operational carbon monoxide retrieval algorithm and selected results for the MOPITT instrument, *J. Geophys. Res.*, *108*(D14), 4399, doi:10.1029/2002JD003186.
- Duncan, B., D. Portman, and C. Spivakovsky (2000), Parameterization of OH for efficient computation in chemical tracer models, *J. Geophys. Res.*, *105*, 12,259–12,262.
- Duncan, B. N., R. V. Martin, A. C. Staudt, R. Yevich, and J. A. Logan (2003), Interannual and seasonal variability of biomass burning emissions constrained by satellite observations, *J. Geophys. Res.*, *108*(D2), 4100, doi:10.1029/2002JD002378.
- Hudman, R. C., et al. (2007), Surface and lightning sources of nitrogen oxides over the United States: Magnitudes, chemical evolution, and outflow, *J. Geophys. Res.*, *112*, D12S05, doi:10.1029/2006JD007912.
- Hudman, R. C., et al. (2008), Biogenic versus anthropogenic sources of CO in the United States, *Geophys. Res. Lett.*, *35*, L04801, doi:10.1029/2007GL032393.
- Kar, J., J. R. Drummond, D. B. A. Jones, J. Liu, F. Nichitju, J. Zou, J. C. Grille, D. P. Edwards, and M. N. Deeter (2006), Carbon monoxide (CO) maximum over the Zagros mountains in the Middle East: Signature of mountain venting, *Geophys. Res. Lett.*, *33*, L15819, doi:10.1029/2006GL026231.
- Lahoz, W. A., Q. Errera, R. Swinbank, and D. Fonteyn (2007), Data assimilation of stratospheric constituents: A review, *Atmos. Chem. Phys.*, *7*, 5745–5773.
- Lamarque, J.-F., B. V. Khattatov, J. C. Gille, and G. P. Brasseur (1999), Assimilation of measurement of Air Pollution from Space (MAPS) CO in a global three-dimensional model, *J. Geophys. Res.*, *104*, 26,209–26,218.
- Lamarque, J.-F., et al. (2004), Application of a bias estimator for the improved assimilation of Measurements of Pollution in the Troposphere (MOPITT) carbon monoxide retrievals, *J. Geophys. Res.*, *109*, D16304, doi:10.1029/2003JD004466.
- Lin, S. J. (2004), A “vertically Lagrangian” finite-volume dynamical core for global models, *Mon. Weather Rev.*, *132*, 2293–2307.
- McMillan, W. W., C. Barnett, L. Strow, M. T. Chahine, M. L. McCourt, J. X. Warner, P. C. Novelli, S. Korontzi, E. S. Maddy, and S. Datta (2005), Daily global maps of carbon monoxide from NASA's Atmospheric Infrared Sounder, *Geophys. Res. Lett.*, *32*, L11801, doi:10.1029/2004GL021821.
- Nedelec, P., J. P. Cammas, and V. Thouret (1998), Measurement of ozone and water vapor by Airbus in-service aircraft: The MOZAIC airborne program, an overview, *J. Geophys. Res.*, *103*, 25,631–25,642.
- Nedelec, P., J. P. Cammas, V. Thouret, G. Athier, J. M. Cousin, C. Legrand, C. Abonne, F. Lecoq, G. Cayez, and C. Marizy (2003), An improved infrared carbon monoxide analyzer for routine measurements aboard commercial Airbus aircraft: Technical validation and first scientific results of the MOZAIC III programme, *Atmos. Chem. Phys.*, *3*, 1551–1564.
- Novelli, P. C., K. A. Masarie, P. M. Lang, B. D. Hall, R. C. Myers, and J. W. Elkins (2003), Reanalysis of tropospheric CO trends: Effects of the

- 1997–1998 wildfires, *J. Geophys. Res.*, *108*(D15), 4464, doi:10.1029/2002JD003031.
- Ott, L. E., J. Bacmeister, S. Pawson, K. Pickering, G. Stenchikov, M. Suarez, H. Huntrieser, M. Loewenstein, J. Lopez, and I. Xueref-Remy (2009), An analysis of convective transport and parameter sensitivity in a single column version of the Goddard Earth Observation System, Version 5. General Circulation Model, *J. Atmos. Sci.*, doi:10.1175/2008JAS2694.1, in press.
- Park, R. J., D. J. Jacob, B. D. Field, and R. M. Yantosca (2004), Natural and transboundary pollution influences on sulfate-nitrate-ammonium aerosols in the United States: Implications for policy, *J. Geophys. Res.*, *109*, D15204, doi:10.1029/2003JD004473.
- Parrish, D. D. (2006), Critical evaluation of U.S. on-road vehicle emission inventories, *Atmos. Environ.*, *40*, 2288–2300.
- Pfister, G., G. Petron, L. K. Emmons, J. C. Gille, D. P. Edwards, J. F. Lamarque, J. L. Attie, C. Granier, and P. C. Novelli (2004), Evaluation of CO simulations and the analysis of the CO budget for Europe, *J. Geophys. Res.*, *109*, D19304, doi:10.1029/2004JD004691.
- Stajner, I., L. P. Riishøjgaard, and R. B. Rood (2001), The GEOS ozone data assimilation system: Specification of error statistics, *Q. J. R. Meteorol. Soc.*, *127*, 1069–1094.
- Stajner, I., et al. (2008), Assimilated ozone from EOS-Aura: Evaluation of the tropopause region and tropospheric columns, *J. Geophys. Res.*, *113*, D16S32, doi:10.1029/2007JD008863.
- Turquety, S., et al. (2007), Inventory of boreal fire emissions for North America in 2004: Importance of peat burning and pyroconvective injection, *J. Geophys. Res.*, *112*, D12S03, doi:10.1029/2006JD007281.
- Yudin, V. A., G. Pétron, J.-F. Lamarque, B. V. Khattatov, P. G. Hess, L. V. Lyjak, J. C. Gille, D. P. Edwards, M. N. Deeter, and L. K. Emmons (2004), Assimilation of the 2000–2001 CO MOPITT retrievals with optimized surface emissions, *Geophys. Res. Lett.*, *31*, L20105, doi:10.1029/2004GL021037.
- Zubrow, A., L. Chen, and V. R. Kotamarthi (2008), EAKF-CMAQ: Introduction and evaluation of a data assimilation for CMAQ based on the ensemble adjustment Kalman filter, *J. Geophys. Res.*, *113*, D09302, doi:10.1029/2007JD009267.
- M. Buchwitz, J. Burrows, and I. Khlystova, Institute of Environmental Physics, University of Bremen, FB1, Otto-Hahn-Allee 1, P.O. Box 33 04 40, D-28334 Bremen, Germany. (michael.buchwitz@iup.physik.uni-bremen.de; burrows@iup.physik.uni-bremen.de; iryna.khlystova@iup.physik.uni-bremen.de)
- R. Hudman, College of Chemistry, University of California, Berkeley, B45 Hilderbrand, Berkeley, CA 94720-1460, USA. (hudman@berkeley.edu)
- P. Nedelec, Laboratoire d'Aérodynamique, Université de Toulouse, CNRS, Observatoire Midi-Pyrénées, 14 Avenue Edouard Belin, F-31400 Toulouse, France. (philippe.nedelec@aero.obs-mip.fr)
- S. Pawson and A. Tangborn, Global Modeling and Assimilation Office, Code 610.1, Goddard Space Flight Center, Greenbelt, MD 20771, USA. (steven.pawson@nasa.gov; andrew.v.tangborn@nasa.gov)
- I. Stajner, Noblis, Inc., 3150 Fairview Park Drive South, MS F540, Falls Church, VA 22042-4519, USA. (ivanka.stajner@noblis.org)